Simulating calcium signals from mice visual cortex with GAN and inferring the functional connectivity of the biological neurons with Spike Neural Network

Mengqi Gao
ShanghaiTech University
gaomq@shanghaitech.edu.cn

Jiachen Wang
ShanghaiTech University
wangjch2@shanghaitech.edu.cn

Hongbo Chen
ShanghaiTech University
chenhb1@shanghaitech.edu.cn

Yuhui Zhong
ShanghaiTech University
zhongyh@shanghaitech.edu.cn

Abstract

Our project lies in the intersection of neural science and computer science, called computational neuroscience. To uncover our brain, two urgent questions are to be answered: how to get more samples and which mathematical tools are appropriate to analyse those data. In this paper, we proposed a method named "neuron-GAN" to produce more neuronal population signals and besides, we proposed and implemented a Spike Neural Network (SNN) with explicit inhibitory neurons and learn-able synaptic weights to infer neural functional connectivity.

The source code can be found here.

1. Introduction

How does our brain perform functional computations? One of the most prestigious forms of this for a life form is associative memory. Without it, individuals could hardly build up concepts about this world. One hypothesis about the generation of intelligence highlights the generalization of associative memory. Since associative learning needs a brain to extract both temporal and spatial features from sensory inputs and to connect items with common features. An abstract concept of this connection is formed in this process, and might indicate a high-level recognition activity.

Paired stimuli are one of the most classical research paradigms for studying associative memory in the neuroscience area. The named milestones to uncover the mechanisms include spike-timing-dependent-plasticity (STDP)[3] , the BCM (Bienenstock-Cooper-Munro) learning rule[4], long-term potentiation (LTP), and long-term depression (LTD). It is worth mentioning that Izhikevich has derived the equivalence of these learning rules[10]. The BCM is the standard algorithm implemented for the LTP/LTD, which directly takes the firing rate of a neuron as input, while STDP focuses on single pairs of spikes. Since the observed neuronal activities in a neural network are the sum of the responses induced by all of the afferent neurons, the classical STDP rule does not apply anymore due to its inability to handle the activities of other afferent neurons. But, as pointed out by Izhikevich, by adding a restriction, we can deduce BCM from STDP. This finding strongly supported a thesis that STDP and LTP/LTD are the performances of the same biological process, and their differences are merely artifacts caused by different observation scales chosen by researchers. More importantly, this work made us one more step closer to a general but precise mathematical model that can describe the brain activities under all observation scales. The canonical neuron model[8] Izhikevich proposed and his other accomplishments[9] in the dynamic system are as great, but due to the page limitations, here is no detailed introduction for these works. One form of the dynamical system describing brain activity can be written as:

$$\dot{v_i} = f_i(v_i) + \epsilon g_i(v_1, \cdots, v_n, \epsilon) \quad \epsilon \ll 1, \quad i = 1, \ldots, n$$

Here v_i is the activity of the ith isolated neuron, f_i describes its dynamics, g_i represents connections converging from other neurons to the ith neuron, and ϵ describes the (dimensionless) strength of synaptic connections[9]. The aforementioned STDP is one example of g_i, and Izhikevich neuron model is one example of f_i. Such a dynamical system is called SNN, which is a special case of recurrent neural network (RNN).

2. Related Work

Previous research[18] published on Science proposed a recurrent neural network based on STDP to explain the cause of the sparsity of the response in the brain to a natural stimulus, and how specific stimuli shape some specific

activity patterns of the network and successfully re-induce them when repeatedly presented to the brain, which means the memory coding in synapses. Recent research[11] used an "implicit" SNN to serve as a computational modal of its conclusions. The protagonist in the so-called prediction from their SNN simulation was "bouts of coincident neural activity", which was visible in the recorded calcium signal and as indistinct as the Hebbian's rule. These examples neither used the data from the wet experiments to train their SNN models, nor required their model to fit the data in a "cell by cell" way. By generating inputs according to prior knowledge, their models are mainly explanatory but rarely predictive.

In this paper, we proposed a SNN based on the Izhikevich neuron model and using nearest-neighbor STDP to perform unsupervised learning of the quantitative connectivity in the biological neural network. Hopefully, such a model with the ability to simulate input neuronal activities with matched cell index and to simulate inter-neuron connections with cell-type specificity could clearly represent the detailed change in the observed biological neural network. Besides, the refined STDP learning rule might serve as an extension for existing SNN libraries[7].

Traditional ways to model neuronal signals includes maximum entropy approaches[17] and dichotomized Gaussian methods [12]. These methods are based on the first-order statistics of the neuronal signals and could not reveal internal patterns in the signals. With the great success of GAN in generation tasks, some researchers also utilize this model-free tool to generate the neuronal signals. Some researchers also directly adopt WGAN to create spike trains[14], while some modified the wave-GAN model to generate calcium imaging [1]. But all these attempts with GANs failed to accurately capture the patterns inside the neural activities and can not generate fully explainable signals.

3. Methods

For the challenges mentioned above, we adopt GAN to augment the calcium signals extracted from behaving mice. The generated signals will be evaluated based on its biological characteristics and their similarities to the original signals. Before searching for the connections between neurons through SNN, we need to use traditional machine learning methods to verify that under 14 categories of different stimulation types, the intensity of calcium signals over time can be multi-classified. We firstly adopted the multi-layer perceptron model, but the classification result was not ideal, whereas the data set gained a better classification result on the SVM. As for the former difficulty, we aim at a specific task: to infer the functional connections of the mice neurons. In this stage, we trained a SNN with the GAN-augmented data, and tried to infer the connections

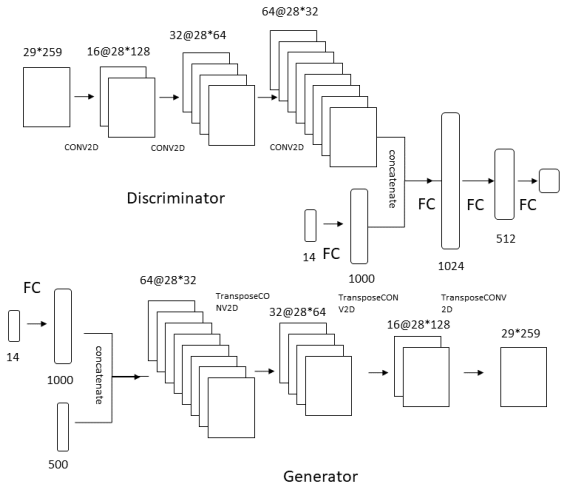

Figure 1: GAN architecture.

between neurons utilizing the structural information of the SNN (such as the weights). The results were evaluated towards the ground truth of the neuronal signal. Through the combination of SNN and classifier, we tried to reconstruct the input neuronal activities and classify different types of stimulus applied on the mice.

3.1. Neuronal Signals Augmentation via GAN

A common behavioral experiments may record the neuronal activities of animals under different stimulus. Given the additives of a population consists of N neurons in time interval Tms under M different stimulus, our goal is synthetic realistic neuronal activities that resemble the recorded signals given one specific stimulus.

In our work, we combine recent advances in GAN communities with biological knowledge to create a new model called "neuro-GAN" to generate neuronal calcium signals. Inspired by recent advances in GAN community, we propose Neuro-GAN, which is capable of generating the fluorescence signal of a neuron population under specific stimulus. The model architecture is shown in 1

The model takes the fluorescence signal of N neurons within T ms and the stimulus type as the input , then output the realistic fluorescence signals that assemble the input.The whole model is based on the classic GAN architecture,and the key features are as follows:

First, we incoporate the stimulus type information to make it a conditional-GAN model[13]. The stimulus is first embeded into an one-hot encoding and then pass one fully connected layer to be combined with the feature map of neuronal population signals.

Second, to extract the spatial activity pattern of neuron populations, we regard each neuron as one channel and use

three convolutional layers[16] to build the feature map.

Lastly, for more stabling training of the Neuro-GAN, we use Wasserstein loss with gradient penalty.

3.2. Neuronal functional connectivity inference via SNN

3.2.1 Specify the inhibitory neurons

We trained a SVM to classify excitatory and inhibitory neurons based on neuronal activity, using special data sets with the ground truth about the neuronal identity provided by our collaborators. The input activity is the fraction change of the neuronal fluorescence. Given by:

$$\Delta F/F_0 = (F_1 - mean(F_0))/mean(F_0)$$

Here F_0 is the signal during the 0.5 seconds before the onset of a stimulus and F_1 is the signal during the 2 seconds after the onset. Only signals with the maximum fraction change above 0.15 were included.

We applied the trained SVM on the data set for SNN (which contains no ground truth about the neuronal identity), and chose 19 neurons as inhibitory neurons specified for SNN, because in the layer II/III of neocortex, only 5%-15% of the total neurons are inhibitory.

3.2.2 SNN Training

We used the Izhikevich neuron model[8] to simulated the dynamics of the observed brain area. The Izhikevich neuron model was described by a set of differential equations:

$$v' = 0.04v^2 + 5v + 140 - u + I$$

$$u' = a(bv - u)$$

$$\text{If } v = 30 \text{ mV}, \quad \text{then } v = c, \quad u = u + d.$$

The input item I is the pre-processed data. The matrix $S = (s_{ij})$ gives the synaptic connection weights between the neurons. And the spiking of neuron$_j$ instantaneously changes the activity of neuron$_i$ (v_i) by s_{ij}. The nearest-neighbor STDP rule was implemented as follows:

$\Delta s_{ij} = s_{ij} * F(\Delta t)$

Here Δt is the spiking-time interval between the neuron that is currently firing and the neuron(s) whose firing time is closest to this moment.

For excitatory to excitatory as well as inhibitory to excitatory connections:

$$F(\Delta t) = \begin{cases} A_p exp(-\Delta t/\tau_p) & \text{if } \Delta t > 0 \\ 0 & \text{if } \Delta t = 0 \\ -A_m exp(\Delta t/\tau_m) & \text{if } \Delta t < 0 \end{cases}$$

τ_p and τ_m are the time constants for synaptic modification, $\tau_p = 20$, $\tau_m = 60$, $A_p = 0.003$, and $A_m/A_p = 0.5$. A_p and A_m determine the maximum amount of synaptic modification. We set these parameters as in [10].

For excitatory to inhibitory connections, the sign of increment was opposite:

$$F(\Delta t) = \begin{cases} -A_p exp(-\Delta t/\tau_p) & \text{if } \Delta t > 0 \\ 0 & \text{if } \Delta t = 0 \\ A_m exp(\Delta t/\tau_m) & \text{if } \Delta t < 0 \end{cases}$$

We made these changes as reported in [5].

4. Experiments

4.1. Neuronal Signals Augmentation via GAN

We trained the Neuro-GAN model on dataset consists of 1500 trials' fluorescence signals with M=14 stimulus for N=259 neurons in T=29 frames.

Both the generator and discriminator are with the WGAN-GP framework, with 5 discriminator update steps for each generator update step. We then used Adam optimizer to optimize both networks, with a learning rate of $\lambda = 10^{-4}, \beta_1 = 0.9$ and $\beta_2 = 0.9999$. The model can be trained on singe-card Tesla V100. The exact hyperparameters being used in this work can be found in(Table 2 .)

Measuring the quality of GAN is always a difficult task, but the fundamental goal is the same: fidelity and diversity. We propose two metrices to evaluate the quality of our Neuro-GAN with clear biological and statistical meanings.

First,in computational Neuroscience, mean firing rate is the most common target for describing neuronal spike signals. It is defined as the number of spikes for neurons during some time. Abundant evidence have shown that the dis-

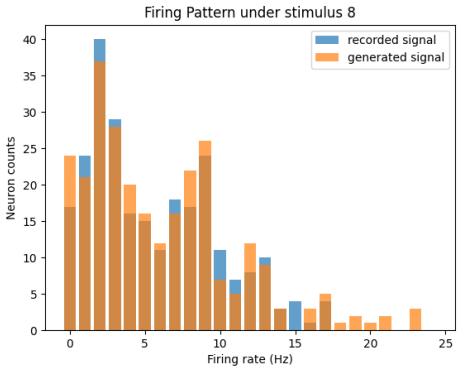

Figure 2: Mean Firing Rate of 259 Neurons under Stimulus 8

Iteration	Inception Score
50	2.37
500	4.86
1000	6.03
5000	6.79
8000	6.80

Table 1: Inception Score during Training

tribution of the mean firing rate among one neuron population is closely related the to its activity patterns.So we first convert the generated fluorescence signals into spike trains with deconvolution algorithms (implemented in OASIS), and then computed the mean firing rate for the synthetic data and recorded data. We randomly sampled the mean firing rate for all 259 neurons in 29 frames under stimulus 8 (which is air-puff in the experiment), and the result is shown in 2.

It is obvious that the distribution of generated signal's firing rate matches the recorded signals. To generalize the above result to all the neuron populations, we compute the Inception Score for all the neurons along training, as show in table 1.

Different from the common IS[2] we seen in visual tasks, there is no pre-trained model like inception-v3. So we first trained a SVM from the recorded data, which reached an accuracy of 88%. We computed the IS from the following formulation:

$$\mathbf{IS}(G) = \exp\left(\mathbb{E}_{\mathbf{x}\sim p_g} D_{KL}(p(y \mid \mathbf{x}) \| p(y))\right)$$

where $p(y \mid x)$, measures how likelyhood of one generated signal belong to the stimulus, represents the fidelity of GAN model. While $p(y)$, is computed from the sample mean of SVM, represents the diversity of the GAN model. In brief, this score should be relatively high for a "good" GAN model and is getting higher during training. From Table 1 we can see that the inception Score increases during the training process and finally end with a high value, which demonstrates that our GAN indeed behaves well.

4.2. Data set Description and Framework

The data set for SNN is the calcium signal of 259 neurons collected by two-photon calcium imaging technology. The original data is videos. Our collaborators circled the neuron cell body on the video as the region of interest (ROI), and then calculated the average brightness in the ROI to obtain the time series data of the fluorescence intensity of each neuron.

4.3. Data Preprocessing

Inspired by[6] and [15], we performed low-pass filtering and differentiating on the raw fluorescence trace. The algorithm formulations of the first-order low-pass filter is as follows:

$$\mathbf{Y(n)} = \alpha \mathbf{X(n)} + (\mathbf{1} - \alpha)\mathbf{Y(n-1)}$$

Here $\alpha, \mathbf{X(n)}, \mathbf{Y(n-1)}, \mathbf{Y(n)}$ stands for the filter coefficient, sample value, last filtered output value and filtered output value respectively.

A key formulation is:

$$\alpha = f \times 2\Pi \times 1/fr$$

Here f means the cut off frequency, which is 0.2 Hz; fr means the frame rate of the raw data, which is 10 Hz.

By analyzing the filtering spectrum of the calcium signal, we found that the frequencies of fundamental signals are generally below about 0.1Hz, so the first-order low-pass filter can meet our requirements when filtering the signal. In this experiment, we used a low-pass filter with a cut-off frequency of 0.2Hz. The comparison between the original signal and the filtered signal is shown in the SI fig.7.

It is not difficult to find that the high frequency noise signal has been eliminated to some extent.

To maintain the ensemble-coding property in the dataset, we added the minimum value of the fluorescence trace, $min(F)$, to the differentiated results, and performed "cell-norm" as [11]. We used SVM to check whether the stimulus-type related features are lost due to the normalization step. We fitted a multi-class model for support vector machines to check whether the stimulus-type related features are lost due to the normalization step. We used the default parameters of the MATLAB 'fitcecoc' function. The pre-processed data set was reshaped to 482 rows and 7511 columns, each row is one observation and each column is one feature. 50 observations were used as the test set and the remaining 432 observations were the training set. The accuracy on the test set was 100%.

We re-scaled the signal to make its standard deviation equal five and then performed gridded interpolation to insert 9 data points between two adjacent data points using the 'pchip' and 'nearest' extrapolation methods.

4.4. Specify the inhibitory neurons

We got 2404 samples from the special data sets, each sample had 25 dimensions. The test set has 240 samples and the training set has 2164 samples. The best SVM we trained has an accuracy about 65%, which used the gaussian kernel with 'BoxConstraint' set to 'Inf' and 'ClassNames' set to [-1 1].

4.5. SNN Training

The output spikes of SNN are shown in SI fig.9. The sum of the number of spikes of each neuron under each type of stimulus showed a similar pattern (SI fig.12) with the

normalized fluorescence signal (SI fig.13), which means the current arguments and the distribution of input data of SNN can restore the signal well.

4.6. Calculate Functional Connection

Following the methods described in [11], we observed in the raw data that a subset of airpuff-responsive neurons (air neurons) showed strong average response with time-locked onset timing to the paired sound-airpuff stimuli (paired stimuli). After the paired stimuli session (SI table.8, stimulus 5-10), these sound-airpuff responsive neurons (audair neurons) showed increased average response to the second round of auditory stimulus (SI fig.14, aud-post). These audair neurons came from the air neurons, and the mechanism underlying their induced response to sound may be the strengthened afferent connection from sound-responsive neurons (aud neurons), which was supported by the increased paired correlation of the activities (SI fig.15) of these audair neurons during the auditory stimulus after paired stimuli. But we did not find increase on the correlation between aud neurons and audair neurons, which might be a result of limited sample number (9 data points from 3*3 neuron pairs).

Assuming the afferent connection was strengthened, we would like to know the role of inhibitory neurons in this process, and calculated the afferent connection from inhibitory neurons to each ensemble using the explicit connection matrix and assigned inhibitory neurons of SNN. The weights of SNN are shown in fig.3, in which the change of weights are visible and within a reasonable range.

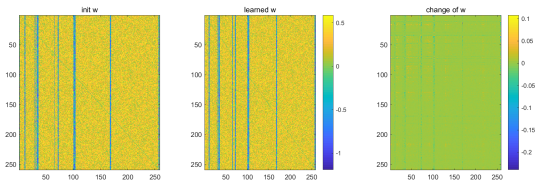

Figure 3: The connection weights in SNN represent the functional connections between observed neurons. w_{ij} is the relative strength of connection from the jth neuron to the ith neuron.

We then calculated the mean and standard error of mean for the connections between neural ensembles of interest. The fraction change (FC) of connection was calculated as

$$FC = (weights_{learned} - weights_{initial})/weights_{initial}$$

And to avoid the randomness between repeated simulations ($n = 50$), before comparing the fraction changes, we normalized the fraction change using the average level of all excitatory neurons.

$$increase = (FC - FC_{Ex})/FC_{Ex}$$

The final answer to our question was that (fig.4 d to f) the mean increase on the afferent connection from aud neurons to audair neurons was close to zero and negative (-0.01), which did not support the original assumption and was unexpected, since the audair neurons were supposed to be related with increased excitatory afferent connections as a direct inference based on the Hebbian's rule. While the mean increase of the the recurrent connection within the audair neurons is 0.30. Then how to account for the appearance of this neural group?

The inhibitory connection to the audair neurons were correlated with the increase on the recurrent connections between audair neurons ($R^2 = 0.61$, fig.5), and were weakly correlated ($R^2 = 0.13$, fig.6) with the increase on the connections from aud neurons to audair neurons. The exact role of the direct inhibition on these paired-stimuli responsive neurons induced by a short-term of paired stimuli is still unclear.

5. Discussion

Our experiments shows that with enough data, modern deep learning technics is capable of generating realistic neuronal population signals, which will greatly benefit the whole neuro-science community. The biggest advantage of our work is that it is based on the generative model, which frees scientists from calculating differenct and complex statistics of neuronal signals (like firing rate or van-rossum distance). In future, it would be a good idea to apply more advanced technics in GAN like style-transfer to help neuro-scientist understand the dynamics of neurons under different stimulus.

How does this increased inhibition work in detail? For example, Is there any relationship between the spiking time point of the audair neurons and that of their afferent inhibitory neurons? The temporal resolution difference between Izhikevich model and calcium signal is several hundred times (1 millisecond v.s. about one second). Though this gap was bridged by interpolation, the SNN input generated by us (SI fig.10) has more zeros and longer tails compared with the gaussian-distributed default input (SI fig.10) set in [8]. This might be the reason for the abnormally high membrane voltage (SI fig.11) of an example neuron, and further influenced the dynamics of our SNN model.

Due to the limited information of the inhibitory neuron identity in this data set, the inhibitory neurons inferred by us could be wrong. Another missing part of prior knowledge is the prior connection between the recorded neurons. In our experiments, we assigned random weights as [8]. These could be uncovered by biological experiments. The most

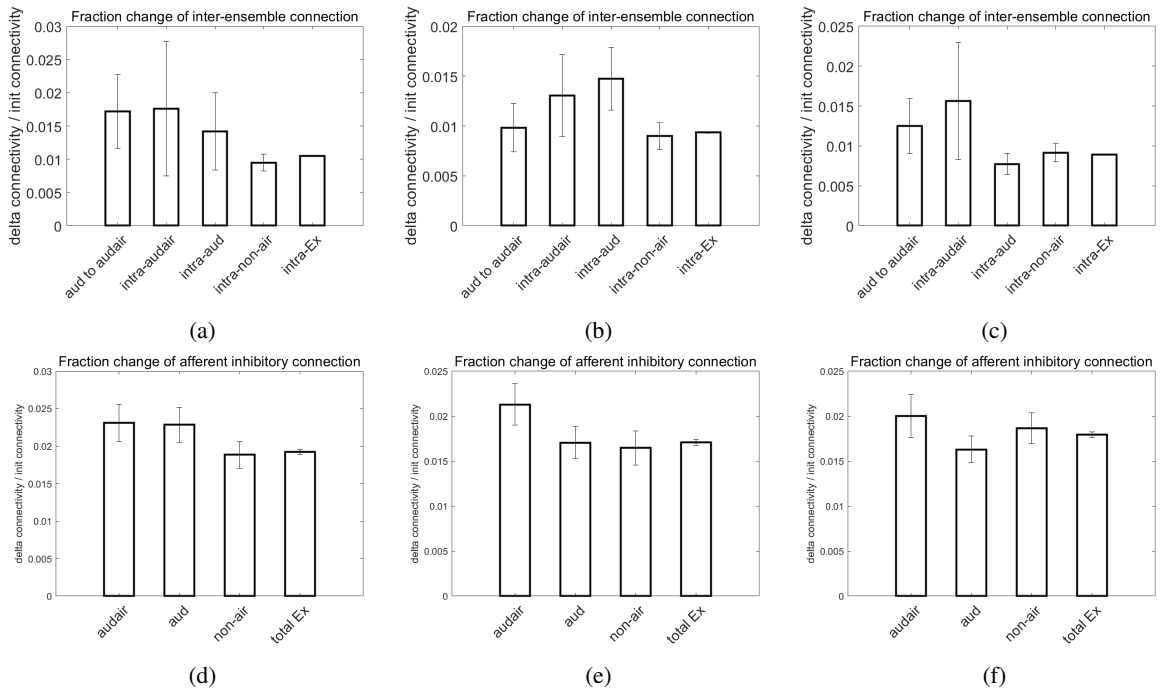

Figure 4: The fraction change of functional connectivity between neural ensembles. a-c:

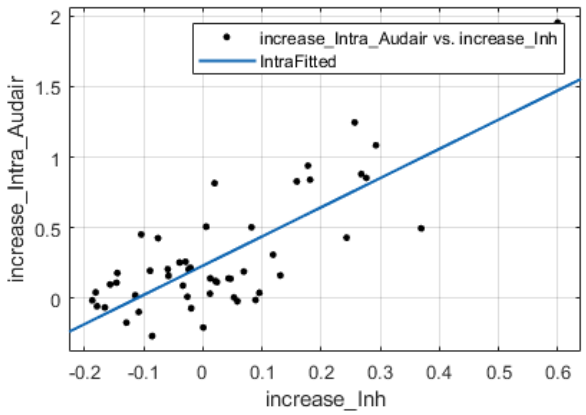

Figure 5: Linear regression between the increase on the recurrent connections of audair neurons and the increase on the inhibitory connections to the audair neurons.

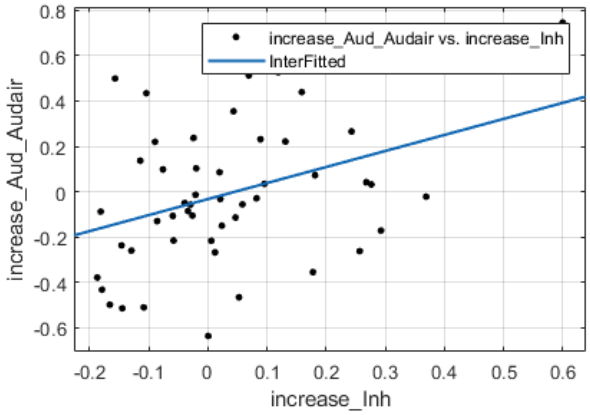

Figure 6: Linear regression of the increase on the connection from aud neurons to audair neurons and the increase on the inhibitory connections to the audair neurons.

important finding in our paper is that SNN can help deriving the connection patterns in the animal brains. In the future, neuroscience community can work together with deep learning community to improve the current model of SNN and incorporate more biological-meaningful structures and functional blocks into it.

Acknowledgements

We would like to thank Prof.Jisong Guan, Dr.Guangyu Wang, Kaiyuan Liu, Chenhui Liu for providing the raw data and sharing their insightful opinions with us.

References

[1] Theoklitos Amvrosiadis, Nathalie Rochefort, Arno Onken, et al. Calciumgan: A generative adversarial network model for synthesising realistic calcium imaging data of neuronal populations. *arXiv preprint arXiv:2009.02707*, 2020. 2

[2] Shane Barratt and Rishi Sharma. A note on the inception score. *arXiv preprint arXiv:1801.01973*, 2018. 4

[3] Guo-qiang Bi and Mu-ming Poo. Synaptic modifications in cultured hippocampal neurons: dependence on spike timing, synaptic strength, and postsynaptic cell type. *Journal of neuroscience*, 18(24):10464–10472, 1998. 1

[4] Elie L Bienenstock, Leon N Cooper, and Paul W Munro. Theory for the development of neuron selectivity: orientation specificity and binocular interaction in visual cortex. *Journal of Neuroscience*, 2(1):32–48, 1982. 1

[5] Natalia Caporale and Yang Dan. Spike timing–dependent plasticity: a hebbian learning rule. *Annu. Rev. Neurosci.*, 31:25–46, 2008. 3

[6] Tsai-Wen Chen, Trevor J Wardill, Yi Sun, Stefan R Pulver, Sabine L Renninger, Amy Baohan, Eric R Schreiter, Rex A Kerr, Michael B Orger, Vivek Jayaraman, et al. Ultrasensitive fluorescent proteins for imaging neuronal activity. *Nature*, 499(7458):295–300, 2013. 4

[7] Hananel Hazan, Daniel J Saunders, Hassaan Khan, Devdhar Patel, Darpan T Sanghavi, Hava T Siegelmann, and Robert Kozma. Bindsnet: A machine learning-oriented spiking neural networks library in python. *Frontiers in neuroinformatics*, 12:89, 2018. 2

[8] EM Izhikevich. Simple model of spiking neurons ieee transactions on neural networks, 2003. 1, 3, 5

[9] E Izhikevich and F Hoppensteadt. Weakly connected neural networks. *New York, NY: Springer. doi*, 10:3–5, 1997. 1

[10] Eugene M Izhikevich and Niraj S Desai. Relating stdp to bcm. *Neural computation*, 15(7):1511–1523, 2003. 1, 3

[11] Thomas Knöpfel, Yann Sweeney, Carola I Radulescu, Nawal Zabouri, Nazanin Doostdar, Claudia Clopath, and Samuel J Barnes. Audio-visual experience strengthens multisensory assemblies in adult mouse visual cortex. *Nature communications*, 10(1):1–15, 2019. 2, 4, 5

[12] Dmitry R Lyamzin, Jakob H Macke, and Nicholas A Lesica. Modeling population spike trains with specified time-varying spike rates, trial-to-trial variability, and pairwise signal and noise correlations. *Frontiers in computational neuroscience*, 4:144, 2010. 2

[13] Mehdi Mirza and Simon Osindero. Conditional generative adversarial nets. *arXiv preprint arXiv:1411.1784*, 2014. 2

[14] Manuel Molano-Mazon, Arno Onken, Eugenio Piasini, and Stefano Panzeri. Synthesizing realistic neural population activity patterns using generative adversarial networks. *arXiv preprint arXiv:1803.00338*, 2018. 2

[15] R Ryley Parrish, Neela K Codadu, Connie Mackenzie-Gray Scott, and Andrew J Trevelyan. Feedforward inhibition ahead of ictal wavefronts is provided by both parvalbumin-and somatostatin-expressing interneurons. *The Journal of physiology*, 597(8):2297–2314, 2019. 4

[16] Alec Radford, Luke Metz, and Soumith Chintala. Unsupervised representation learning with deep convolutional generative adversarial networks. *arXiv preprint arXiv:1511.06434*, 2015. 3

[17] Aonan Tang, David Jackson, Jon Hobbs, Wei Chen, Jodi L Smith, Hema Patel, Anita Prieto, Dumitru Petrusca, Matthew I Grivich, Alexander Sher, et al. A maximum entropy model applied to spatial and temporal correlations from cortical networks in vitro. *Journal of Neuroscience*, 28(2):505–518, 2008. 2

[18] Tim P Vogels, Henning Sprekeler, Friedemann Zenke, Claudia Clopath, and Wulfram Gerstner. Inhibitory plasticity balances excitation and inhibition in sensory pathways and memory networks. *Science*, 334(6062):1569–1573, 2011. 1

6. Appendix

Hyper-parameters of Neuro-GAN:

Hyper-parameteres	Values
Noise Dimension	500
Critic Update	5
λ gradient penalty	10
Batch Size	32
Learning Rate	0.0001

Table 2: Comparison of 5 methods

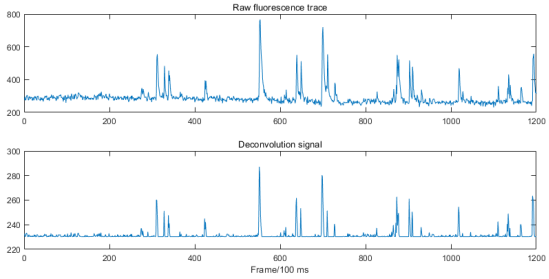

Figure 7: Filtered data of neuron 58 under stimulus 4

Session	Stimulus type(Abbr.)	Repeat times
1	NO stimulus (bas)	-
2	blue light (vis)	39
3	sound (aud)	40
4	airpuff (air)	38
5	vis_aud	34
6	aud_vis	34
7	vis_air	27
8	air_vis	28
9	aud_air	35
10	air_aud	26
11	vis	40
12	aud	40
13	air	36
14	bas	-

Figure 8: The order of stimulus applied to this mouse. Each stimulus was repeatedly given with 3 seconds inter trial interval. Session 5-10 are paired stimuli: during these sessions, two stimuli with 200 ms inter stimulus interval were applied in one trial.

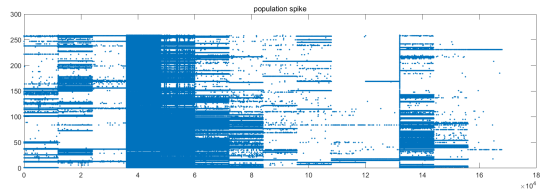

Figure 9: All spikes of SNN during the training process.

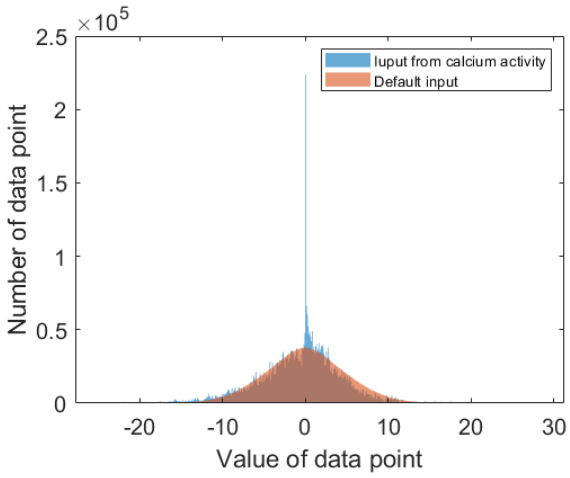

Figure 10: The histogram of input generated from calcium signal (blue) or the default input of Izhikevich model (red).

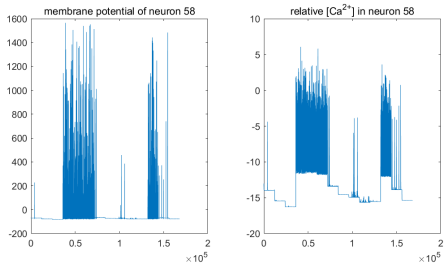

Figure 11: The membrane potential (left) and relative calcium concentration (right) in neuron 58 during one training process. The membrane potential is supposed to be lower than 100 mV in physiological condition.

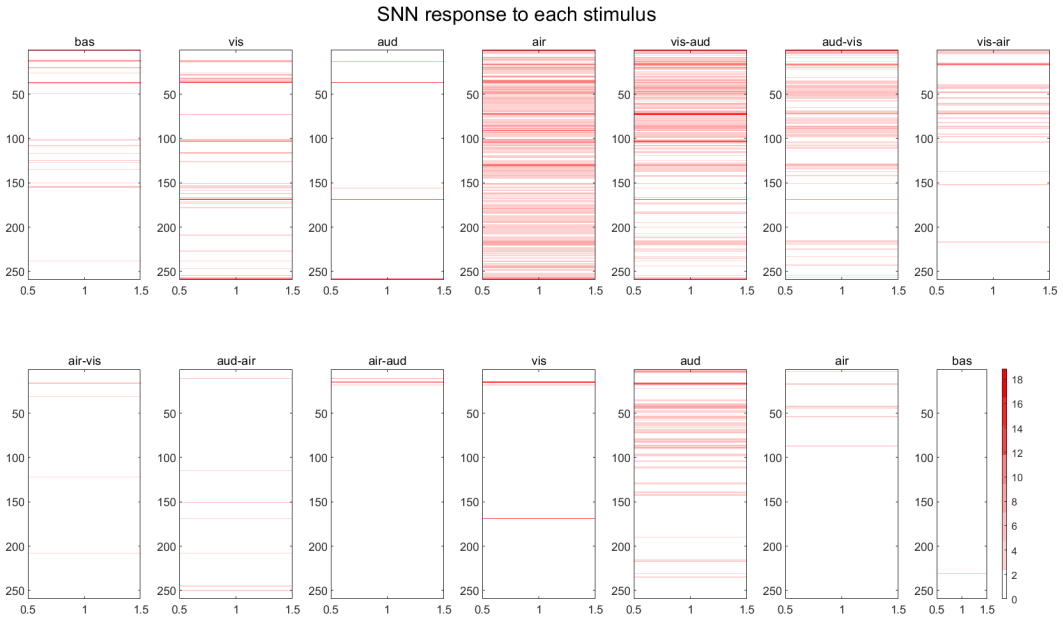

Figure 12: Average response of SNN to each stimulus.

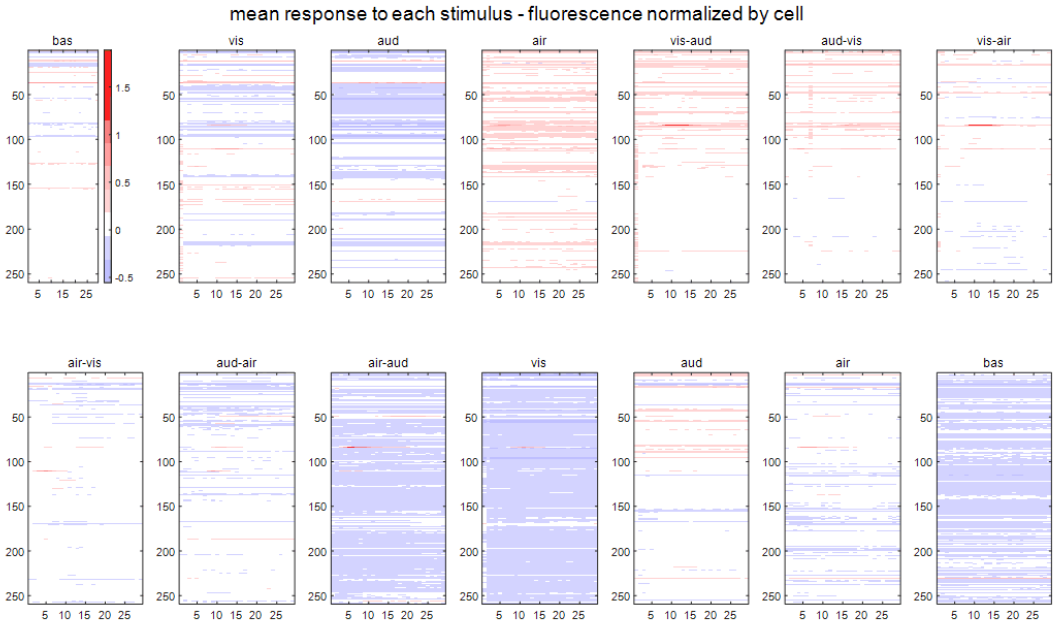

Figure 13: Average signal of raw data under each stimulus.

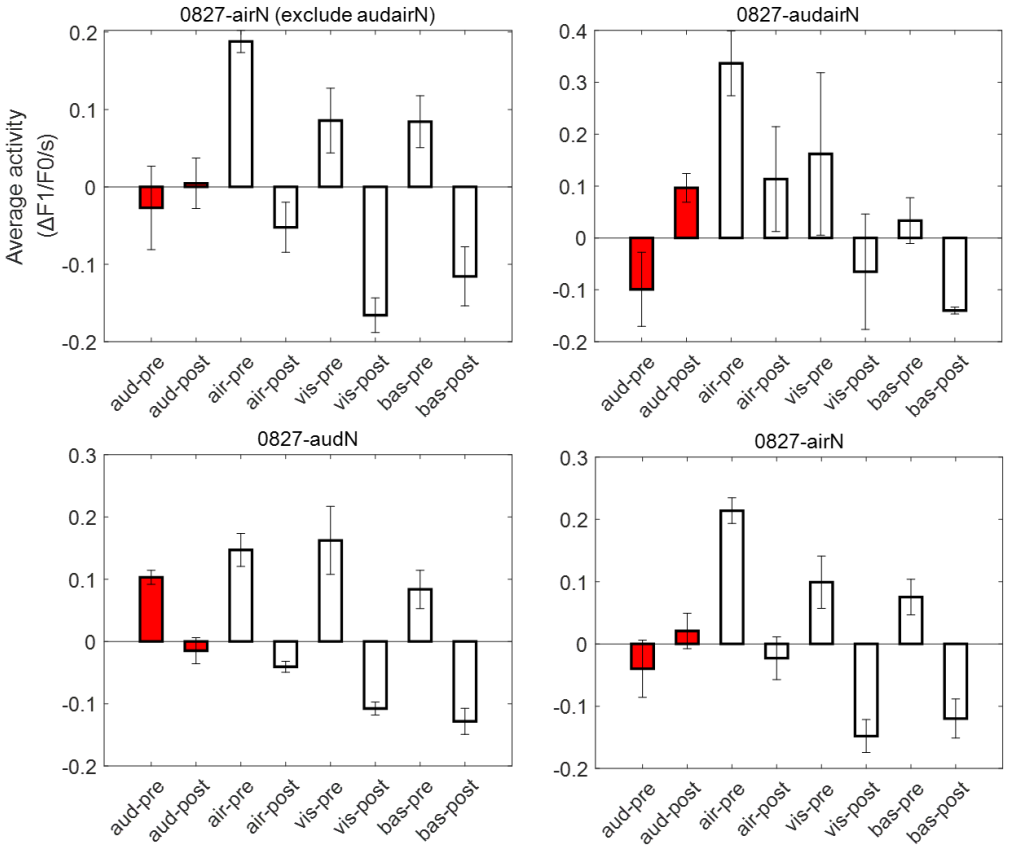

Figure 14: The audair neurons (the right-up figure) showed increased responses to sound after the paired stimuli.

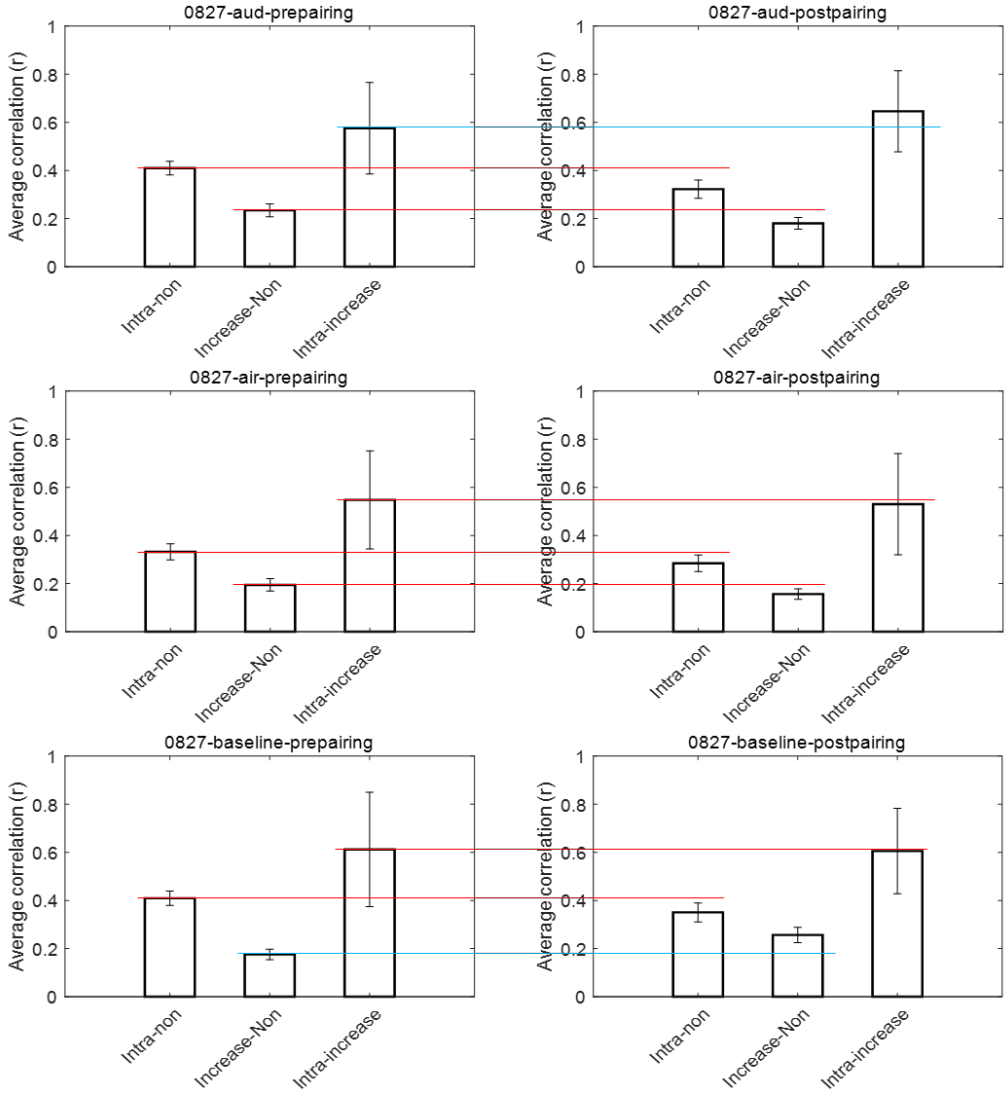

Figure 15: The sound-airpuff responsive neurons (audair neurons) showed increased correlation with each other under auditory stimulus after the paired stimuli. The correlation between neural ensemble activities under different stimulus condition. Intra-non: the paired correlation between neurons that are responsive to airpuff but not sound-airpuff. Intra-increase: the paired correlation between neurons that are responsive to both airpuff and sound-airpuff. Increase-Non: the paired correlation between these two neural ensembles but not within each group. Row 1: the mouse is under sound stimulus. Row 2: the mouse is under airpuff stimulus. Row 3: the mouse is under no stimulus; record the baseline neural activity. Red line: decreased correlation. Blue line: increased correlation.